

Synthesis, Spectral, Characterization, DFT and Biological Studies of New 3-[(3-Chlorophenyl)-hydrazono]-pentane-2,4-dione Metal Complexes

Sadeek. A. Sadeek*, Wael. A. Zordok, Ahmed. F. El-Farargy, and Sameh. I. El-Desoky†

Department of Chemistry, Faculty of Science, Zagazig University, Zagazig, Egypt.

*E-mail: s_sadeek@zu.edu.eg

†Department of Quality Control, Ceramica Royal, Egypt

(Received November 6, 2013; Accepted January 24, 2014)

ABSTRACT. A new series of metal complexes of V(IV), Pd(II), Pt(IV), Ce(IV) and U(VI) with 3-[(3-chlorophenyl)-hydrazono]-pentane-2,4-dione (Cphpd) were synthesized and characterized by elemental analysis, molar conductivity, magnetic moment measurements, UV-vis, FT-IR and ¹H NMR as well as TG-DTG techniques. The data indicated that the Cphpd acts as a bidentate ligand through the hydrazono nitrogen and one keto oxygen. The kinetic parameters have been evaluated by using Coats Redfern (CR) and Horowitz-Metzger (HM) methods. The thermodynamic data reflected the thermal stability for all complexes. The calculated bond length and the bond stretching force constant, F(U=O), values for UO₂ bond are 0.775 Å and 286.95 Nm⁻¹. The bond lengths, bond angles, dipole moment and the lowest energy model structure of the complexes have been determined with DFT calculations. The antimicrobial activity of the synthesized ligand and its complexes were screened.

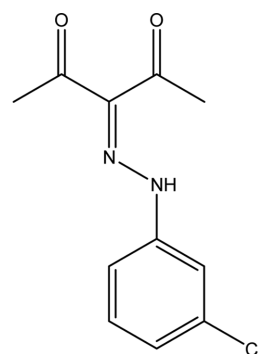
Key words: Cphpd, Transition metal complexes, FT-IR, Mass spectra

INTRODUCTION

Recently, chlorinated organic compounds have attracted attention due to the ability of chlorine to act as polar hydrogen or hydroxyl mimic. Therefore, substitution of hydrogen by chlorine has been a strategy in designing molecules for biological activity studies.¹ Benzenediazonium chloride is excellent starting material for the synthesis of 3-[(3-chlorophenyl)-hydrazono]-pentane-2,4-dione (Cphpd) (Scheme 1) via the reaction of 3-chlorobenzenediazonium chloride with acetyl acetone.¹

In recent years the chemistry of heterocyclic compounds are well known for their diverse therapeutic properties and exhibited antibacterial, anticancer, antiulcer, diuretics, anticonvulsant, antihypertensive, antitumor, antifungal, anti-AIDS and antiviral properties.² Metal chelates play an important role in various fields of chemical, biological and technological sciences on coordination, ligands might improve their bioactivity profiles, while some inactive ligand may acquire pharmacological properties. Activity of various anti-inflammatory drugs existing in market has enhanced after complexation with transition metal ion.³

A detailed literature research has shown that no work is reported on the 3-[(3-chlorophenyl)-hydrazono]-pentane-2,4-dione (Cphpd). Thus, our aim was to synthesize and characterize the complexes of V(IV), Pd(II), Pt(IV), Ce(IV) and U(VI) with Cphpd in order to investigate their mag-



3-[(3-chloro-phenyl)-hydrazono]-pentane-2,4-dione

Scheme 1.

netic, spectroscopic and thermal techniques in an attempt to examine the mode of binding. Density functional theory (DFT) was used to compute the cation type influence on theoretical parameters of V(IV), Pd(II), Pt(IV) and Ce(IV) complexes and detect the exact structure of these complexes. Indeed, the biological activity of the ligand and its complexes were screened against selected kinds of bacteria and fungi.

EXPERIMENTAL

Materials

All chemicals used for the preparation of the complexes were of analytical reagent grade, commercially available

from different sources and used without further purification.

Synthesis

Synthesis of metal complexes

The black solid complex $[\text{VO}(\text{Cphpd})_2(\text{H}_2\text{O})]\text{SO}_4$ was prepared by adding 1 mmol (0.18 g) of $\text{VO}(\text{SO}_4)_2 \cdot \text{H}_2\text{O}$ in 20 ml acetone drop-wisely to a stirred clear solution of Cphpd (2 mmol, 0.48 g) at room temperature for one day. The solution was left for slow evaporation, the black precipitate formed was filtered off, washed with doubly distilled water several times and dried in vacuum over CaCl_2 in a desiccator. The deep-brown, olive-green and brown solid complexes of $[\text{Pd}(\text{Cphpd})_2(\text{H}_2\text{O})_2]\text{Cl}_2 \cdot 2\text{H}_2\text{O}$, $[\text{Pt}(\text{Cphpd})_2\text{Cl}_2]\text{Cl}_2$, $[\text{Ce}(\text{Cphpd})_2(\text{H}_2\text{O})_2](\text{SO}_4)_2$ and $[\text{UO}_2(\text{Cphpd})_2](\text{NO}_3)_2 \cdot 3\text{H}_2\text{O}$ were prepared in a similar manner described above by using acetone as a solvent and using PdCl_2 , PtCl_4 , $\text{Ce}(\text{SO}_4)_2$ and $\text{UO}_2(\text{NO}_3)_2 \cdot 6\text{H}_2\text{O}$ respectively, in 1:2 molar ratio (M: Cphpd). All compounds were characterized by their elemental analysis, molar conductance, magnetic moment, IR, ^1H NMR, electronic, mass spectra as well as thermal analysis.

Instrumentation-Physical Measurements

C, H and N analyses was carried out on a Perkin Elmer CHN 2400. The percentage of the metal ions were determined gravimetrically by transforming the solid products into metal oxide or sulphate and also determined by using atomic absorption method. Spectrometer model PYE-UNICAM SP 1900 fitted with the corresponding lamp was used for this purpose. IR spectra were recorded on FT-IR 460 PLUS (KBr discs) in the range from $4000\text{--}400\text{ cm}^{-1}$, ^1H NMR spectra were recorded on Varian Mercury VX-300 NMR Spectrometer using DMSO-d_6 as solvent. TGA-DTG measurements were carried out with heating rate being controlled at $10\text{ }^\circ\text{C min}^{-1}$ under N_2 atmosphere from room temperature to $800\text{ }^\circ\text{C}$ using TGA-50H Shimadzu. The mass of sample was accurately weighted out in an aluminum crucible. Electronic spectra were obtained using UV-3101PC Shimadzu. The solid reflection spectra were recorded with KBr pellets. Magnetic measurements were carried out on a Sherwood scientific magnetic balance using Gouy method using $\text{Hg}[\text{Co}(\text{SCN})_4]$ as calibrant. Melting points were determined on an Electrothermal-9100 apparatus. Molar conductivities of the solution of the ligand and metal complexes in DMSO at $1 \times 10^{-3}\text{ M}$ were measured on CONSORT K410.

Biological Activity

Antibacterial activity of the ligands and their metal

complexes was investigated by a modied method of Beecher and Wong,⁴ against different bacterial species, such as *S. aureus* K1, *B. subtilis* K22, *E. Coli* K32 and *P. aeruginosa* SW1. And antifungal screening was studied against two species, *aspergillus flavus* (*A. flavus*) and *aspergillus fumigates* (*A. fumigates*), the tested microorganisms isolates were isolated from Egyptian soil and identified according to the standard mycological and bacteriological keys for identification of fungi and bacteria as stock cultures in the microbiology laboratory, Faculty of Science, Zagazig University. The nutrient agar medium for antibacterial was Müller–Hinton agar (30.0% beef extract, 1.75% Casein hydrolysate, 0.15% starch and 1.7% agar) and for antifungal (3% Sucrose, 0.3% NaNO_3 , 0.1% K_2HPO_4 , 0.05% KCl, 0.001% FeSO_4 , 2% Agar-Agar) was prepared and then cooled to $47\text{ }^\circ\text{C}$ and seeded with tested microorganisms. After solidification 5 mm diameter holes were punched by a sterile cork-borer. The investigated compounds, i.e., ligands and their complexes were introduced in holes (only $100\text{ }\mu\text{L}$) after being dissolved in DMSO at 10^{-3} M . These culture plates were then incubated at $37\text{ }^\circ\text{C}$ for 20 h for bacteria and seven days at $30\text{ }^\circ\text{C}$ for fungi. The activity was determined by measuring the diameter of the inhibition zones (in mm). Growth inhibition was calculated with reference to the positive control, i.e., ligands.

RESULTS AND DISCUSSION

The complexes of 3-[(3-chlorophenyl)-hydrazono]-pentane-2,4-dione (Cphpd) with V(IV), Pd(II), Pt(IV), Ce(IV) and U(VI) were synthesized and studied. Single x-ray diffraction measurements could not be done due to the formation of non suitable crystals. The stoichiometry of the complexes was established on the basis of their elemental analysis (Table 1). The formulas pattern and the geometry of the complexes were assigned on the basis of physico-chemical parameters such as conductance measurements, magnetic susceptibilities and spectral measurements. The magnetic susceptibility measurements for all the five complexes indicated that the complexes were found as diamagnetism except V(IV) and Pd(II) complexes have magnetic moments of 1.73 and 3.00 B.M. at room temperature, respectively. The molar conductance values of Cphpd and their metal complexes measured in DMSO at room temperature were found from 2.14 to $234.59\text{ S cm}^2\text{ mol}^{-1}$ (Table 1). The molar conductance values showed that all the complexes were electrolytes.⁵ Qualitative reactions for the isolated complexes indicated the presence of sulphate, chloride and nitrate ions as counter ions which agreed well with the

Table 1. Elemental analysis and physico-analytical data for Cphpd and its metal complexes

Compounds M.Wt. (M.F.)	Yield%	Mp/°C	Color	Found (Calcd.) (%)					μ_{eff} (B.M)	Λ (S cm ² mol ⁻¹)
				C	H	N	Cl	M		
Cphpd 238.50, C ₁₁ H ₁₁ N ₂ O ₂ Cl	–	110	Buff	55.27 (55.34)	4.59 (4.61)	11.71 (11.74)	14.80 (14.88)	–	Diamagnetic	2.14
[VO(C ₁₁ H ₁₁ N ₂ O ₂ Cl) ₂ (H ₂ O)]SO ₄ 658, VC ₂₂ H ₂₄ N ₄ O ₁₀ Cl ₂ S	73	119	Black	39.99 (40.12)	3.53 (3.64)	8.39 (8.51)	10.66 (10.79)	7.64 (7.74)	1.73	109.69
[Pd(C ₁₁ H ₁₁ N ₂ O ₂ Cl) ₂ (H ₂ O) ₂]Cl ₂ ·2H ₂ O 726.42, PdC ₂₂ H ₃₀ N ₄ O ₈ Cl ₄	90	120	Deep-brown	36.29 (36.34)	4.03 (4.12)	7.63 (7.70)	19.49 (19.54)	14.55 (14.64)	3.00	163.71
[Pt(C ₁₁ H ₁₁ N ₂ O ₂ Cl) ₂ Cl ₂]Cl ₂ 814.08, PtC ₂₂ H ₂₂ N ₄ O ₄ Cl ₆	78.6	140	Deep-brown	32.31 (32.42)	2.59 (2.70)	6.77 (6.87)	26.06 (26.16)	23.77 (23.96)	Diamagnetic	160.33
[Ce(C ₁₁ H ₁₁ N ₂ O ₂ Cl) ₂ (H ₂ O) ₂](SO ₄) ₂ 845.12, CeC ₂₂ H ₂₆ N ₄ O ₁₄ Cl ₂ S ₂	64	120	Olive-green	31.12 (31.23)	3.03 (3.07)	6.51 (6.62)	8.35 (8.40)	16.38 (16.57)	Diamagnetic	227.50
[UO ₂ (C ₁₁ H ₁₁ N ₂ O ₂ Cl) ₂](NO ₃) ₂ ·3H ₂ O 925.03, UC ₂₂ H ₂₈ N ₆ O ₁₅ Cl ₂	81.4	198	Brown	28.58 (28.60)	3.00 (3.03)	9.07 (9.10)	7.55 (7.69)	25.67 (25.78)	Diamagnetic	234.59

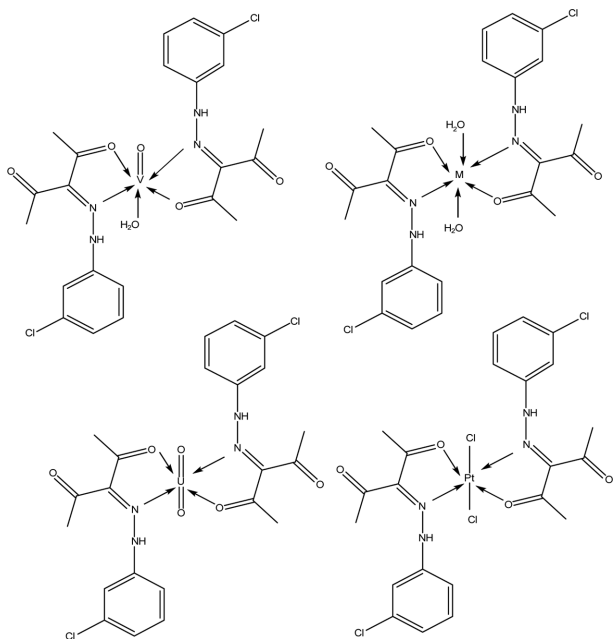
results of molar conductance and infrared data.

Spectroscopic Studies

IR absorption spectra

Before discussing the assignments of the infrared spectra of the free ligand (Cphpd) and its metal complexes, the proposed structures of the complexes must be considered. Here, metal ions reacted with Cphpd forming complexes of monomeric structure where the metal ions are six coordinated.

The proposed structure of $[M(\text{Cphpd})_2(\text{H}_2\text{O})_2]^{+n}$ (M = Pd(II) and Ce(IV)), $[\text{Pt}(\text{Cphpd})_2\text{Cl}_2]^{+2}$ and $[\text{UO}_2(\text{Cphpd})_2]^{+2}$ complexes, (Scheme 2), contain only a plane of symmetry



Scheme 2. The proposed coordination mode of V(IV), Pt(IV), U(VI) and M=Pd(II) and Ce(IV) with Cphpd.

and hence the four complexes may belong to C_s symmetry but V(IV) complex may belong to C_1 .⁶⁻¹⁴ The C_s complexes are expected to display 177 for Pd(II) and Ce(IV) and 165 for Pt(IV) and U(VI) vibrational fundamentals and all vibrations are distributed between motions of the types A^{I} and A^{II} , all are monodegenerate, infrared and Raman active. The data showed that the $\nu_{\text{as}}(\text{U}=\text{O})$ and $\nu_{\text{s}}(\text{U}=\text{O})$ absorption bands occur at 941 and 822 cm^{-1} as a very strong singlet and strong bands, respectively. These assignments for the stretching vibrations of the uranyl group, agreed quite well with those known for many dioxouranium (VI) complexes.^{7,9,15,16} The $\nu(\text{U}=\text{O})$ of the uranyl unit in the $[\text{UO}_2(\text{Cphpd})_2]^{+2}$ complex occurred at lower frequency values compared with those for the same unit, UO_2 , in simple salts and this was consistent with the formation of the complex.⁷ The $\nu_{\text{s}}(\text{U}=\text{O})$ value was used to calculate both the bond length and the bond stretching force constant, $F(\text{U}=\text{O})$, for UO_2 bond in our complex according to known methods.^{7,9} The calculated bond length and force constant values are 0.775 Å and 286.95 Nm^{-1} , respectively.

The infrared spectrum of free ligand shows two bands at 1490 and 1670 cm^{-1} which attributed to the stretching vibration of $\nu(\text{C}=\text{N})$ for hydrazono group and $\nu(\text{C}=\text{O})$ for two equivalent keto groups.^{9,10} Upon comparison of the IR spectra of the complexes with those of free ligand the shift of $\nu(\text{C}=\text{N})$ to higher frequency values (1508 and 1512 cm^{-1}) confirming that the ligand molecule coordinated to metal ion through the nitrogen atom of hydrazono group. The shift of $\nu(\text{C}=\text{N})$ to higher frequency values may indicate an increase of C=N bond strength upon coordination.⁷⁻¹¹ The possibility that the electron density on the nitrogen atom was decreased upon coordination to metal ions means a decrease in the electron repulsion between the nitrogen lone pair and the double bond electrons leading to a stronger C=N

bond then, a higher frequency bond. Also, the shift of $\nu(\text{C}=\text{O})$ to lower frequency value (1632 and 1639 cm^{-1}) in the spectra of the complexes may indicate a decrease of the $\text{C}=\text{O}$ bond strength upon coordination.⁹ The bands in the range $3489\text{--}3400\text{ cm}^{-1}$ in the spectra of the complexes can be attributed to the $\nu(\text{O}-\text{H})$ vibration of the water molecules.¹¹ The $\nu(\text{N}-\text{H})$ vibration appears in the region of $3310\text{--}3222\text{ cm}^{-1}$ and the stretching vibrations $\nu(\text{C}-\text{H})$ of phenyl and methyl groups are assigned as a number of bands in the region $3178\text{--}2920\text{ cm}^{-1}$.¹²

The spectra of the isolated solid complexes showed a group of new bands with different intensities which characteristics for $\nu(\text{M}-\text{O})$ and $\nu(\text{M}-\text{N})$. The $\nu(\text{M}-\text{O})$ and $\nu(\text{M}-\text{N})$ bands observed at 632 , 590 and 522 cm^{-1} for V(IV), at 683 , 625 and 590 cm^{-1} for Pd(II), at 679 , 575 and 448 cm^{-1} for Pt(II), at 667 , 533 and 489 for Ce(IV) and at 683 , 625 and 590 cm^{-1} for U(VI) (Table S3) which are absent in the spectrum of Cphpd.⁶⁻¹²

Electronic spectra

The UV-visible spectral data of the free ligand (Cphpd) and its metal complexes were recorded (Table 2). The electronic absorption spectrum of the Cphpd was reflected by three absorption bands at 262 , 281 and 374 . The first band at 262 nm may be attributed to $\pi-\pi^*$ (phenyl ring) transition and the second two bands are assigned to $n-\pi^*$ ($-\text{NH}$, $-\text{C}=\text{O}$ and $-\text{C}=\text{N}$) transition, these transitions occur in case of unsaturated hydrocarbons which contain ketone and cyanide group.¹⁷ The intraligand bands were slightly shifted to longer wavelength (bathochromic shift) and to lower values (hypsochromic shift) upon complexation and the presence of new bands in the reflection spectra of all complexes indicated the formation of their metal complexes. The new bands in the range from 419 to 499 nm may be

assigned to the ligand to metal charge-transfer.^{18,19} The electronic spectra of V(IV), Pd(II) and Pt(IV) complexes showed bands from 515 to 579 nm . These bands were assigned to d-d transitions.

Nuclear magnetic resonance (¹H NMR)

The ¹H NMR spectra of Cphpd and its metal complexes confirms the suggested structures. The proton of $-\text{NH}$ signal for the Pt(IV), Ce(IV) and U(VI) complexes observed at δ : 14.53 ppm (s, 2H, $-\text{NH}$, exchange with D_2O) showed no big differences as compared to that of the free ligand at δ : 13.24 ppm (s, 1H, $-\text{NH}$, exchange with D_2O). This enhances the hypothesis that $-\text{NH}$ is not the coordinating group. The new signals are observed in the range δ : $3.24\text{--}3.51\text{ ppm}$ due to presence of H_2O molecules in all complexes. On the other hand, the values of protons of $-\text{CH}$ aliphatic observed in the range of $2.07\text{--}2.58\text{ ppm}$ (s, 12H, $-\text{CH}_3$) and those of aromatic ring in the range of $6.81\text{--}7.88\text{ ppm}$ (m, 8H, $\text{Ar}-\text{H}$) increased and the intensity of signals is increased, as shown in Table 3.²⁰ From ¹H NMR and FT-IR results, it was proposed that the Cphpd coordinated to the central metal ion as bidentate ligand through the nitrogen atom of hydrazono group and oxygen atom of one keto group.²¹

Thermal studies

Thermogravimetric (TGA) and differential thermogravimetric (DTG) analyses for Cphpd and its metal complexes were carried out. Table 4 gives the maximum temperature values for decomposition along with the corresponding weight loss values for each step of the decomposition reaction. The Cphpd is thermally stable up to $135\text{ }^\circ\text{C}$ and the decomposition started at $135\text{ }^\circ\text{C}$ and finished at $550\text{ }^\circ\text{C}$ with one stage at one maximum $205\text{ }^\circ\text{C}$ and is accompanied by a weight loss of 59.54% (Fig. S4(A)).

Table 2. UV-vis spectral data of the free ligand Cphpd and its metal complexes

Assignments (nm)	Cphpd	Metal complexes with				
		V(IV)	Pd(II)	Pt(IV)	Ce(IV)	U(VI)
$\pi-\pi^*$ transitions	262	272	252	259	210, 233	248
$n-\pi^*$ transitions	281, 374	291, 394	364	292, 370	314	381, 386
Ligand-metal charge transfer	–	439, 493	459, 499	419, 438	495	475, 483
d-d transitions	–	524, 566	577	515, 522, 579	–	–

Table 3. Selected ¹H NMR data (in ppm) of Cphpd and its diamagnetic metal complexes

Compounds	δH ; $-\text{CH}$ aliphatic (methyl)	δH ; H_2O	δH ; $-\text{CH}$ aromatic	δH ; $-\text{NH}$ hydrazid
Cphpd	2.42	–	6.81–7.23	13.24
Pt(IV) / Cphpd	2.08–2.58	3.51	7.19–7.86	14.53
Ce(IV) / Cphpd	2.44–2.51	3.46	7.20–7.88	14.53
U(VI) / Cphpd	2.07–2.57	3.24–3.37	7.20–7.87	14.54

Table 4. Thermogravimetric data of Cphpd and its metal complexes

Compounds	Decomposition	DTG _{max} (°C)	% Estimated (calculated)		Assignment
			Mass loss	Total mass loss	Lost species
Cphpd 238.50, C ₁₁ H ₁₁ N ₂ O ₂ Cl	First step Residue	205	59.54 (59.75) 40.46 (40.25)	59.54 (59.75)	CH ₄ +2CO+NH ₄ Cl+NH ₃ 8C
[VO(C ₁₁ H ₁₁ N ₂ O ₂ Cl) ₂ (H ₂ O)]SO ₄ 658, VC ₂₂ H ₂₄ N ₄ O ₁₀ Cl ₂ S	First step Residue	228	75.57 (75.83) 24.43 (24.15)	75.57 (75.83)	10C ₂ H ₂ +2HCl+4NO+CO+H ₂ O VSO ₄ +C
[Pd(C ₁₁ H ₁₁ N ₂ O ₂ Cl) ₂ (H ₂ O) ₂]Cl ₂ .2H ₂ O 726.42, PdC ₂₂ H ₃₀ N ₄ O ₈ Cl ₄	First step Second step Residue	56 205, 466	4.83 (4.96) 61.54 (61.67) 33.63 (33.37)	66.37 (66.63)	2H ₂ O 6C ₂ H ₂ +4HCl+2NH ₃ +NO ₂ +NO+2H ₂ O PdO+10C
[Pt(C ₁₁ H ₁₁ N ₂ O ₂ Cl) ₂ Cl ₂]Cl ₂ 814.08, PtC ₂₂ H ₂₂ N ₄ O ₄ Cl ₆	First step Residue	215	66.37 (66.21) 33.63 (33.79)	66.37 (66.21)	8C ₂ H ₂ +2CO+6HCl+2N ₂ PtO ₂ +4C
[Ce(C ₁₁ H ₁₁ N ₂ O ₂ Cl) ₂ (H ₂ O) ₂](SO ₄) ₂ 845.12, CeC ₂₂ H ₂₆ N ₄ O ₁₄ Cl ₂ S ₂	First step Residue	211, 498	56.69 (56.44) 43.31(43.55)	56.69 (56.44)	9C ₂ H ₂ +CO ₂ +2NO ₂ + 3NH ₄ Cl Ce(SO ₄) ₂ +3C
[UO ₂ (C ₁₁ H ₁₁ N ₂ O ₂ Cl) ₂](NO ₃) ₂ .3H ₂ O 925.03, UC ₂₂ H ₂₈ N ₆ O ₁₅ Cl ₂	First step Second step Residue	81 198, 490	5.62 (5.83) 56.03 (55.89) 38.35 (38.27)	61.65 (61.72)	3H ₂ O 7C ₂ H ₂ +CO ₂ +4NO ₂ +2NH ₄ Cl UO ₂ +7C

The thermal decomposition of [VO(Cphpd)₂(H₂O)]SO₄ complex proceeds with one degradation step. The decomposition stage occurs at one maximum temperature at 228 °C with intermediate formation of very unstable products which were not identified and the weight loss found at this stage equals to 75.57% corresponds to loss 10C₂H₂+2HCl+4NO+CO+H₂O.

For Pd(II) complex, the thermal decomposition exhibits two main degradation steps. The first step involves decomposition in which the complex losses water molecules of crystallization. The second step of decomposition occurs at two maxima 205 and 466 °C with a weight loss of 61.54% associated with the loss of Cphpd and two coordinated water molecules, leaving palladium oxide as residue.

The thermal degradation exhibits one step with maximum temperature at 215 °C for [Pt(Cphpd)₂Cl₂]Cl₂ and two maxima at 211 and 498 °C for [Ce(Cphpd)₂(H₂O)₂](SO₄)₂ with a weight loss of 8C₂H₂+2CO+6HCl+2N₂ (66.37%) and 9C₂H₂+CO₂+2NO₂+3NH₄Cl (56.69%), giving PtO₂ and Ce(SO₄)₂ as a final product.

For U(VI) complex, the thermal decomposition exhibits two main degradation steps. The first step occurring from 35 to 85 °C is accompanied by a weight loss of 5.62% in agreement with the theoretical values 5.83% for the loss of three uncoordinated water molecules. The second stage occurs at two maxima temperatures 198 and 490 °C corresponding to the loss of Cphpd forming uranium oxide as a final product (Table 4).

Biological Activities

The susceptibility of certain strains of bacterium, such as *S. aureus* K1, *B. subtilis* K22, *E. Coli* K32 and *P. aeruginosa* SW1 and antifungal screening was studied against

two species, *aspergillus flavus* (*A. flavus*) and *aspergillus fumigates* (*A. fumigates*) towards Cphpd and its complexes, and judged by measuring size of the inhibitions diameter (Table 5). The results of the antibacterial study of Cphpd and the five metal complexes have inhibitory action against all four types of bacteria and no antifungal activity observed for ligand and their metal complexes. The complex of V(IV) showed a significant difference against all four types of bacteria than free ligand. The Pd(II) complex showed significant for Gram-negative and highly significant for Gram-positive bacteria. Pt(IV) showed highly significant difference against *E. Coli* K32, significant difference against *S. aureus* K1 and not significant against *B. subtilis* K22 and *P. aeruginosa* SW1. The Ce(IV) showed highly significant against Gram-positive and not significant against Gram-negative bacteria. U(VI) showed highly significant difference against *S. aureus* K1, significant difference against *E. Coli* K32 and *B. subtilis* (Table 5). The results are promising compared with the previous studies.^{21,22} Such increased activity of metal chelate can be explained on the basis of the oxidation state of the metal ion, overtone concept and chelation theory. According to the overtone concept of cell permeability, the lipid membrane that surrounds the cell favors the passage of only lipid-soluble materials in which liposolubility is an important factor that controls the antimicrobial activity. On chelation the polarity of the metal ion will be reduced to a greater extent due to overlap of ligand orbital and partial sharing of the positive charge of the metal ion with donor groups. Further it increases the delocalization of π -electrons over the whole chelate ring and enhances the lipophilicity of the complexes.²³ This increased

Table 5. The inhibition diameter zone values (mm) for Cphpd and their complexes

Compounds	Microbial species						
	Bacteria				fungi		
	<i>E. coli</i>	<i>P. aeruginosa</i>	<i>B. subtilis</i>	<i>S. aureus</i>	<i>A. flarvus</i>	<i>A. Fumigates</i>	
Cphpd	10±0.33	15±0.11	20±0.22	23±0.90	0	0	
Cphpd / V(IV)	20 ⁺ ±0.22	24 ⁺ ±0.02	26 ⁺ ±0.44	28 ⁺ ±0.06	0	0	
Cphpd / Pd(II)	21 ⁺ ±0.11	25 ⁺ ±0.03	35 ⁺ ±0.30	38 ⁺ ±0.88	0	0	
Cphpd / Pt(IV)	25 ⁺ ±0.22	18 ^{NS} ±0.04	22 ^{NS} ±0.20	28 ⁺ ±0.33	0	0	
Cphpd / Ce(IV)	14 ^{NS} ±0.15	16 ^{NS} ±0.05	30 ⁺ ±0.13	40 ⁺ ±0.11	0	0	
Cphpd / U(VI)	18 ⁺ ±0.12	0	25 ⁺ ±0.60	39 ⁺ ±0.14	0	0	
VO(SO ₄) ₂ .2H ₂ O	0	0	0	0	0	0	
PdCl ₂	9±0.73	0	5±0.53	0	0	0	
PtCl ₄	0	0	0	0	0	0	
Ce(SO ₄) ₂	0	0	0	0	0	0	
UO ₂ (NO ₃) ₂ .6H ₂ O	0	0	0	0	0	0	
Control (DMSO)	0	0	0	0	0	0	
Standard	Ampicilin	0	13	28	18	0	0
	Amoxycillin	0	23	22	16	0	0
	Cefaloxin	24	0	27	0	0	0

Statistical significance P^{NS}-P not significant, P>0.05; P⁺-P significant, P<0.05; P⁺-P highly significant, P<0.01; P⁺-P very highly significant, P>0.001; Student's t-test (Paired).

lipophilicity enhances the penetration of complexes into the lipid membranes and blocks the metal binding sites in enzymes of microorganisms. These complexes also disturb the respiration process of the cell and thus block the synthesis of proteins, which restricts further growth of the microorganisms.

COMPUTATIONAL DETAILS

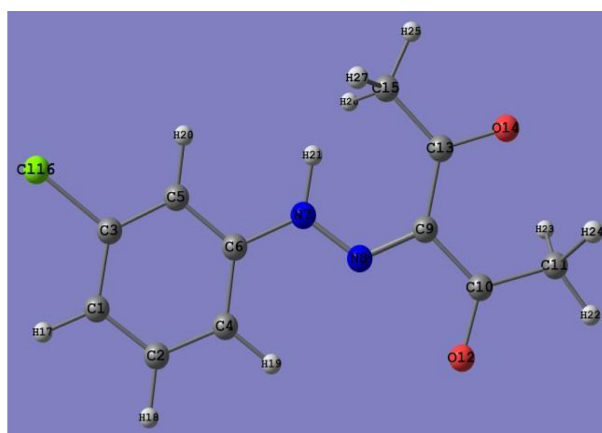
Computational Method

The geometric parameters and energies were computed by density functional theory at the B3LYP/CEP-31G level of theory, using the GAUSSIAN 98W package of the programs, on geometries that were optimized at CEP-31G basis set. The high basis set was chosen to detect the energies at a highly accurate level. The atomic charges were computed using the natural atomic orbital populations. The B3LYP is the keyword for the hybrid functional,²⁴ which is a linear combination of the gradient functionals proposed by Becke²⁵ and Lee, Yang and Parr,²⁶ together with the Hartree-Fock local exchange function.²⁷

Structural Parameters and Model of Ligand Cphpd

The biological activity of Cphpd is mainly determined by its fine structure, the Cphpd has many characteristic structural features. The antimicrobial activity of the synthesized Cphpd might be attributed to interference with nutrient transporter

on plasma membrane as ABC transporter, or changing the ionic state by free chlorine/metal interaction with membrane poreins/interference with membrane lipids. As well as, the reliable cytotoxic effect reasons, might be due to the interaction with various metallo-enzymes especially with mitochondrial enzymes.²⁸ Table 6 gives the optimized geometry of Cphpd as obtained from B3LYP/CEP-31G calculations. The values of bond distances are compared nicely with that obtained from X-ray data.²⁹ The molecule is not highly sterically-hindered, the two benzene ring in the same plane of the all fragments. This observation is supported by the values of calculated dihedral angles. Scheme 3, showed the opti-



Scheme 3. Optimized geometrical structure of Cphpd by using B3LYP/CEP-31G.

Table 6. Equilibrium geometric parameters bond lengths (Å), bond angles (°), dihedral angles (°) and charge density of Cphpd ligand by using DFT/B3LYP/CEP-31G.

Bond length (Å)			
C13–O14	1.285 (1.30)	C10–O12	1.285 (1.30)
C10–C11	1.463	C13–C15	1.469
C9–C10	1.452 (1.41)	C9–N8	1.334
C6–N7	1.406	C2–C4	1.392 (1.38)
C3–C1	1.737	C1–C2	1.395
C5–C6	1.401	C5–C6	1.401
C3–C5	1.388	C1–C3	1.389
N7–N8	1.304	C4–C6	1.402
		C9–C13	1.449
Bond angle (°)			
C6N7N8	121.22	C9C13O14	117.69
N7N8C9	121.83	C9C13C15	124.06
C15C13O14	118.25	C9C10C11	119.07
N8C9C10	112.82	C11C10O12	120.58
N8C9C13	124.41		
Dihedral angles (°)			
C5C6N7N8	–180.00	N8C9C10O12	0.00
N8C9C13O14	–180.00	N8C9C10C11	180.00
N8C9C13C15	0.00		
Charges			
N8	–0.143	O14	–0.372
C10	0.323	C9	–0.09
C13	0.302	O12	–0.386
N7	–0.013	C15	–0.215
C11	–0.212		
Total energy/au		–149.1178	
Total dipole moment/D		3.023	

mized geometrical structure of Cphpd molecule. The dihedral angles confirm C10O12 group is lying in cis form with respect to C9N8 group and C13O14 group in trans form with respect to C9N8 group. The chelation of this ligand can be occurred through the nitrogen atom of hydrazono group N8 and the oxygen atom of keto group O12 as bi-dentate ligand.

Charge distribution on the optimized geometry of Cphpd is given in Table 6. There is a significant built up of charge density on the oxygen atoms of the two keto groups and nitrogen atom of hydrazono group so we expect that Cphpd ligand behave as bi-dentate (O_{keto} and N_{hyd} atoms) and the molecule is not highly dipole $\mu=3.023$ because the planarity of the Cphpd molecule, the charges accumulated on O12 and O14 are -0.386 and -0.372 , respectively, also, the charges on N_8 and N_7 are -0.143 and 0.013 , respectively. These values of charges enhance the chelation through the O12 of keto group and the N_8 of the hydrazono group. The value of energy of the optimized geometry is -149.117 au.

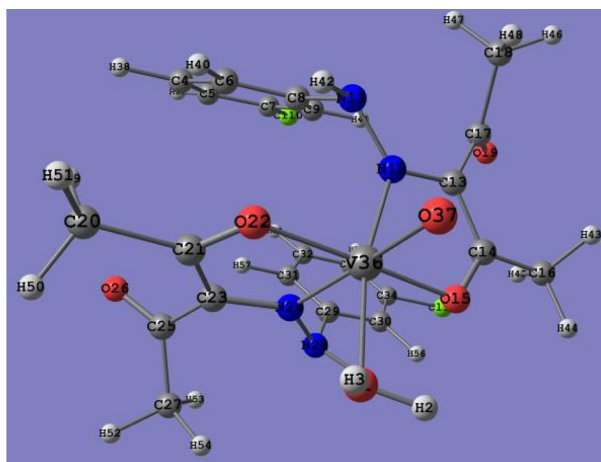
Proposal Structure of the Complexes with Molecular Modeling

Description of the structure of $[\text{VO}(\text{Cphpd})_2(\text{H}_2\text{O})]^{2+}$

The V(IV) may be chelated with two molecules of Cphpd through four coordinate bonds (O_{keto} and N_{hyd} atoms) from each molecule. The experimental data set that the result complex is six-coordinate so, the complex consists of four coordinate bonds with two Cphpd molecules and coordinated bond with water molecule beside oxygen atom of V(IV) ion. In this part we study theoretically the structure parameters of $[\text{VO}(\text{Cphpd})_2(\text{H}_2\text{O})]^{2+}$ complex. The energy of the isomers is almost equal as expected,³⁰ it is difficult to distinguish between *trans* and *cis* isomers. Nevertheless, the *trans* Oc-isomer exhibit the lowest energy.

The structure of complex with atomic numbering scheme is shown in Scheme 4. The complex consists of two units of Cphpd molecule and one water molecule with VO ion. The complex is six-coordinate with distorted octahedral environment around the metal ion. The bond lengths and angles were calculated and found in Table 7. These values agree with these expected for a distorted octahedron.^{31–36} The two Cphpd molecules are perpendicular to each other and they are not lying in the same plane.

The energy of this complex is -338.096 au and the dipole moment is high (17.865D) and the charges accumulated on O_{keto} are -0.274 and -0.255 and on N_{hyd} are 0.04 and 0.019, in octahedral complex. There is a strong interaction between central metal ion V(IV) which has charge equal $+0.578$ and Cphpd molecule which more negative oxygen and nitrogen atoms in octahedral complex. For this reason the octahedral complex is more stable.



Scheme 4. Optimized geometrical structure of *trans* Oc-isomer of $[\text{VO}(\text{Cphpd})_2(\text{H}_2\text{O})]^{2+}$ complex by using B3LYP/CEP-31G.

Table 7. Equilibrium geometric parameters bond lengths (Å), bond angles (°) and charge density of $[\text{VO}(\text{Cphpd})_2(\text{H}_2\text{O})]^{2+}$ complex by using B3LYP/CEP-31G

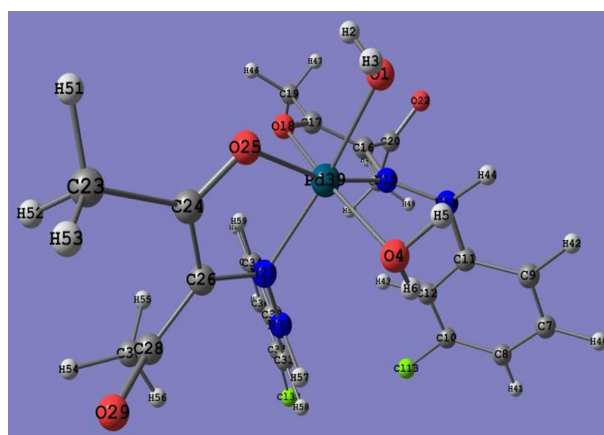
Bond length (Å)			
V–O15	1.869	C13–N12	1.349
V–O22	1.868	C44–O15	1.215
V–N12	1.914	C23–N24	1.348
V–N24	1.912	C21–O22	1.215
V–O37	1.789	C13–C14	1.364
V–O _{H2O}	1.899	C21–C23	1.364
Bond angle (°)			
O37 V O15	92.72	O15 V O1	88.37
O37 V N12	88.13	O15 V O37	92.72
O37 V N24	166.19	N12 V N24	102.39
O37 V O22	88.92	N12 V O22	100.18
O37 V O1	86.53	N12 V O1	167.31
O15 V N12	80.39	N24 V O22	80.49
O15 V N24	97.81	N24 V O1	84.86
O15 V O22	178.29	O22 V O1	91.23
		O22 V O37	88.92
Charges			
V	0.578	C21	0.381
O15	–0.274	C23	0.012
N12	0.040	O37	–0.281
C13	0.019	O1	–0.322
N24	0.006	C14	0.419
		O22	–0.255
Total energy/au		–338.096	
Total dipole moment/D		17.856	

Description of the structure of $[\text{Pd}(\text{Cphpd})_2(\text{H}_2\text{O})_2]^{2+}$

Scheme 5 shows the optimized geometrical structure of $[\text{Pd}(\text{Cphpd})_2(\text{H}_2\text{O})_2]^{2+}$ with the atomic numbering scheme. The selected bond distances and angles are given in Table 8.

The Pd(II) ion, at a crystallographic inversion center, is in a distorted octahedral environment. The metal ion may be coordinated by two oxygen atoms (O_{keto}) and two nitrogen atoms (N_{hyd}) of two Cphpd ligand beside two oxygen atoms of two water molecules to complete the octahedral structure.^{37–46}

In the equatorial plane the Pd(II) bonded with one oxygen atom and one nitrogen atom (O18 and N15) of Cphpd molecule beside two oxygen atoms, one oxygen atom (O25) of other ligand molecule and one oxygen atom (O4) of water molecule. These four atoms are lying in the same plane which perpendicular to the other plane occupied by other atoms (N27) of other ligand molecule and O1 of other water molecule. The bond angles O18PdO25 and O18PdN27 are 93.48 and 96.75. The bond angles N15PdO25 and O18PdO4 are 166.32 and 170.52, also, the bond angle O1PdN27 is 159.51. These values confirm that the two ligand molecules not occupy the same plane but they are perpendicular to

**Scheme 5.** Optimized geometrical structure of trans O-isomer of $[\text{Pd}(\text{Cphpd})_2(\text{H}_2\text{O})_2]^{2+}$ complex by using B3LYP/CEP-31G.**Table 8.** Equilibrium geometric parameters bond lengths (Å), bond angles (°) and charge density of $[\text{Pd}(\text{Cphpd})_2(\text{H}_2\text{O})_2]^{2+}$ by using DFT/B3LYP/CEP-31G

Bond length (Å)			
Pd–O18	1.923	Pd–O4	1.951
Pd–O25	1.924	C17–O18	1.216
Pd–N15	1.967	C16–C17	1.363
Pd–N27	1.971	C16–N15	1.348
Pd–O1	1.953	C24–O25	1.214
C26–N27	1.349	C24–C26	1.364
Bond angle (°)			
O1 Pd N15	86.49	O18 Pd N27 N27	96.75
O1 Pd O25	82.49	Pd O25 O1 Pd	79.08
N15 Pd N27	112.95	O18	93.21
N15 Pd O25	166.32	O1 Pd O4	87.26
O18 Pd O25	93.48	N27 Pd O4	85.85
N15 Pd O4	91.56	O1 Pd N27	159.51
O18 Pd O4	170.52	N15 Pd O18	79.03
O25 Pd O4	95.96		
Charges			
Pd	0.688	C17	0.401
C16	0.131	C24	0.402
N27	0.559	O4	–0.395
O1	–0.399	O18	–0.568
N15	0.689	O25	–0.660
		C26	0.137
Total energy/au		–363.135	
Total dipole moment/D		8.097	

each other. The energy of this complex is –363.135 au and the dipole moment is high 8.097D, so this complex is more stable.

The bond distances between Pd(II) and surrounded oxygen atoms and nitrogen atoms of Cphpd in complex are shown in Table 8. Also, the charges accumulated on O_{keto} are –0.568 and –0.660 and on N_{hyd} are 0.689 and 0.559. There is a strong interaction between central metal ion Pd(II)

which has charge equal +0.688 and more negative oxygen and nitrogen atoms in octahedral complex. For this reason the octahedral complex is more stable and Pd(II) favor coordinated with two molecules of Cphpd with four coordinated bonds and completes the octahedron structure by bonding with two water molecules.

CONCLUSION

The reaction of some transition metal ions V(IV), Pd(II), Pt(IV), Ce(IV) and U(VI) with Cphpd has been studied. The results of the elemental analysis and thermogravimetric analysis deduced the formation of 2:1 Cphpd/metal ions complexes in all cases. The structure of the formed complexes were further supported by infrared, UV-vis and ^1H NMR spectra. The Cphpd has two donating centers O_{keto} and N_{hyd} when chelated with metal ions and the metal ions completed the octahedral structures with water molecules or chloride ions, there are six-coordinated bonds are formed four with two Cphpd molecules and other two with two water molecules or chloride ions. The produced complexes are treated as distorted octahedral complex. For all studied complexes the two Cphpd molecules are perpendicular to each other and they are not lying in the same plane. In case of V(IV) in VO ion the energy difference between two enantiomers *cis* and *trans* is very low, it is difficult to distinguish between *trans* or *cis* isomers. Nevertheless, the *trans*-isomer exhibits the lowest energy value. Antimicrobial studies were carried out against *S. aureus* K1, *B. subtilis* K22, *E. coli* K32 and *P. aeruginosa* SW1 and antifungal screening was studied. The results showed significant increase in antibacterial activity of metal complexes as compared with uncomplexed ligand and no antifungal activity observed for ligand and their complexes.

Acknowledgments. The author would like to thank the colleagues at University of Zagazig, Faculty of Science, Microbiology and Chemistry Department for performing the antimicrobial measurements (Prof. Dr. Ashraf sabry and Dr. Walaa H. El-Shwiniy). And the publication cost of this paper was supported by the Korean Chemical Society.

REFERENCES

1. Odabasoglu, M.; Büyükgüngör, O.; Sarojini, B. K.; Narayana, B. *Acta Cryst.* **2007**, *E63*, o4135.
2. Rashad, A. E.; Shamroukh, A. H.; El-Hashash, M. A.; El-Faragy, A. F.; Yousif, N. M.; Salama, M. A.; Mostafa, A.; El-Shahat, M. *J. Heterocyclic. Chem.* **2012**, *49*, 1130.
3. Zordok, W. A.; Sadeek, S. A.; EL-Shwiniy, W. H. *J. Coord. Chem.* **2012**, *65*, 353.
4. Beecher, D. J.; Wong, A. C. *Appl. Environ. Microbiol.* **1994**, *60*, 1646.
5. Geary, W. J. *Coord. Chem. Rev.* **1971**, *7*, 81.
6. Nour, E. M.; Alnami, I. S.; Alem, N. A. *J. Phys. Chem. Solids* **1992**, *53*, 197.
7. Mcglynnm, S. P.; Smith, J. K.; Neely, W. C. *J. Chem. Phys.* **1961**, *35*, 105.
8. Syamal, A.; Singhal, P. O.; Banerjee, S. *Synth. React. Inorg. Met.-Org. Chem.* **1980**, *243*, 10.
9. Jones, L. H. *Spectrochim. Acta* **1958**, *10*, 395; Jones, L. H. *Spectrochim. Acta* **1959**, *11*, 409.
10. Nakamoto, K. *Infrared and Raman Spectra of Inorganic and Coordination Compounds*, 4th ed.; Wiley: New York, 1986, pp 230–233.
11. Sultana, N.; Arayne, M. S.; Gul, S.; Shamim, S. *J. Mol. Struct.* **2010**, *975*, 285.
12. Zordok, W. A.; El-Shwiniy, W. H.; El-Attar, M. S.; Sadeek, S. A. *J. Mol. Struct.* **2013**, *1047*, 267.
13. King, D. E.; Malone, R.; Lilley, S. H. *Am. Fam. Phys.* **2000**, *61*, 2741.
14. Patai, S. *Chemistry of the Carbon-nitrogen Double Bond*; Wiley: New York, 1970; pp 238–247.
15. Jones, L. H. *Spectrochim. Acta* **1959**, *15*, 409.
16. Sadeek, S. A.; Teleb, S. M.; AL-Kority, A. M. *J. Indian Chem. Soc.* **1993**, *70*, 63.
17. Refat, M. S. *Spectrochim. Acta., Part A* **2007**, *68*, 1393.
18. Nakamoto, K.; McCarthy, P. J.; *Spectroscopy and Structure of Metal Chelate Compounds*; John Wiley & Sons: New York, London, Sydney, 1968; chapter 2.
19. Saif, M.; Mashaly, M. M.; Eid, M. F.; Fouad, R. *Spectrochim. Acta.; Part A* **2012**, *92*, 347.
20. Skauge, T.; Turel, I.; Sletten, E. *Inorg. Chem. Acta.* **2002**, *339*, 239.
21. Rossmore, H. W. *Disinfection, Sterilization and Preservation*, 4th ed.; Block, S. S., Ed., Lea and Febiger: Philadelphia, 1991; pp 290–321.
22. Russell, A. D. *Disinfection, Sterilization and Preservation*, 4th ed.; Block, S. S., Ed., Lea and Febinger: Philadelphia, 1991, pp. 27–59.
23. Beltagi, A. M. *J. Pharm. Biomed. Anal.* **2003**, *31*, 1079.
24. Kohn, W.; Sham, L. J. *Phys. Rev. A* **1965**, *140*, 1133.
25. Becke, A. D. *Phys. Rev. A* **1988**, *38*, 3098.
26. Lee, C.; Yang, W.; Parr, R. G. *Phys. Rev. B* **1988**, *37*.
27. Flurry, R. L. Jr. *Molecular Orbital Theory of Bonding in Organic Molecules*; Marcel Dekker: New York, 1968.
28. Warrilow, A. G. S.; Martel, C. M.; Parker, J. E.; Melo, N.; Lamb, D. C.; Nes, W. D.; Kelly, D. E.; Kelly, S. L. *Antimicrob. Agents Chemother.* **2010**, *54*, 4235.
29. Turel, I.; Golic, L.; Bukovec, P.; Gubina, M. *J. Inorg. Biochem.* **1998**, *71*, 53.
30. Ahmed, M.; Schwendt, P.; Marek, J.; Sivak, M. *Polyhedron* **2004**, *23*, 655.
31. Grivani, G.; Khalaji, A. D.; Tahmasebi, V.; Gotoh, K.; Ishida,

- H. *Polyhedron* **2012**, *31*, 265.
32. Gonzalez-Baro, A. C.; Castellano, E. E.; Piro, O. E.; Parajon-Costa, B. S. *Polyhedron* **2005**, *24*, 49.
33. Kuriakose, M.; Prathapachandra Kurup, M. R.; Suresh, E. *Polyhedron* **2007**, *26*, 2713.
34. Vannan, M.; Lloffman, J. T.; Dimayuga, V. L.; Dwight, T.; Carrano, C. J. *Inorg. Chem. Acta* **2007**, *360*, 529.
35. Rochon, F. D.; Massarweh, G. *Inorg. Chim. Acta* **2006**, *359*, 4095.
36. Quintal, S. M. O.; Felix, V.; Drew, M. G. B.; Nogueira, H. I. S. *Polyhedron* **2006**, *25*, 753.
37. Hao, Y. Z.; Li, Z. X.; Tian, J. L. *J. Mol. Catal. A.: Chem.* **2007**, *265*, 258.
38. Kaplum, M.; Sandstrom, M.; Bostrom, D.; Shchukarev, A.; Persson, P. *Inorg. Chem. Acta* **2005**, *358*, 527.
39. López, C.; Caubet, A.; Perez, S.; Solans, X.; Font-Bardia, M. *J. Organ. Chem.* **2003**, *681*, 82.
40. Kumar, P. R.; Upreti, S.; Singh, A. K. *Polyhedron* **2008**, *27*, 1610–1622.
41. Al-Jibori, S. A.; Habeeb, A. T.; Al-Jibori, G. H. H.; Dayaaf, N. A.; Merzweiler, K.; Wagner, C.; Schmidt, H.; Hogarth, G. *Polyhedron* **2014**, *67*, 338.
42. Sanchez, G.; Garcia, J.; Meseguer, D.; Serrano, J. L.; Garcia, L.; Perez, J.; Lopez, G. *Inorg. Chim. Acta* **2004**, *357*, 4568.
43. Griffith, D. M.; Bíró, L.; Platts, J. A.; Müller-Bunz, H.; Farkas, E.; Buglyó, P. *Inorg. Chim. Acta* **2012**, *380*, 291.
44. Oltean, D.; Pöllnitz, A.; Silvestru, A. *Polyhedron* **2013**, *53*, 67.
45. Gao, H. L.; Yi, L.; Zhao, B.; Zhao, X. Q.; Cheng, P.; Liao, D. Z.; Yan, S. P. *Inorg. Chem.* **2006**, *45*, 5980.
46. Aghabozorg, H.; et al. *Polyhedron* **2010**, *29*, 1453.
-